NOTICE: When government or other drawings, specifications or other data are used for any purpose other than in connection with a definitely related government procurement operation, the U. S. Government thereby incurs no responsibility, nor any obligation whatsoever; and the fact that the Government may have formulated, furnished, or in any way supplied the said drawings, specifications, or other data is not to be regarded by implication or otherwise as in any manner licensing the holder or any other person or corporation, or conveying any rights or permission to manufacture, use or sell any patented invention that may in any way be related thereto.

NRL Report 5601

CURVES OF ATMOSPHERIC-ABSORPTION LOSS FOR USE IN RADAR RANGE CALCULATION

L. V. Blake

Search Radar Branch
Radar Division

March 23, 1961

$2.60

627 400

U. S. NAVAL RESEARCH LABORATORY
Washington. D.C.

CONTENTS

Abstract	ii
Problem Status	ii
Authorization	ii
INTRODUCTION	1
THE VAN VLECK THEORY	4
Equation for Oxygen Absorption	4
Equation for Water-Vapor Absorption	6
OUTLINE OF CALCULATION PROCEDURE	8
DISCUSSION OF RESULTS	10
ACKNOWLEDGMENTS	11
REFERENCES	12
APPENDIX A - Derivation of an Approximation for the Absorption by Oxygen	13
APPENDIX B - Some Details and Numerical Results of the Calculations	15
APPENDIX C - Application to Radar Range Calculation	22

ABSTRACT

The attenuation of radar signals due to absorption by atmospheric oxygen and water vapor has been calculated for a surface-based radar as a function of the target range and elevation angle, for frequencies in the range 100 to 10,000 megacycles, employing the theory of Van Vleck. The results are presented in the form of curves that are especially adapted to use in calculating radar maximum range. Limitations of the theory, particularly in the assignment of values to the line-breadth factors and in the details of the collision-broadening formulas are discussed. It is concluded that these limitations are not likely to produce serious errors. Comparison is made with attenuation calculations made by others for ray paths through the entire atmopshere.

PROBLEM STATUS

The work described in this report is a part of a more comprehensive and continuing project. This is a final report on this phase of the report.

AUTHORIZATION

NRL Problem R02-05
Projects RF 001-02-41-4001 and SF 001-02-02
BuShips No. S-1914

Manuscript submitted January 12, 1961.

CURVES OF ATMOSPHERIC-ABSORPTION LOSS FOR USE IN RADAR RANGE CALCULATION

INTRODUCTION

To calculate the range of a radar system, or the signal strength at a distant point for any radio system, it is necessary to know the amount of loss incurred by absorption in the propagation medium. If the propagation path is in the earth's atmosphere, this loss is due primarily to the oxygen and water-vapor molecules, when there is no precipitation.

The theory of radio-wave absorption by oxygen and water vapor has been worked out by Van Vleck (1,2). By means of his equations the absorption per unit distance may be calculated as a function of the wavelength, pressure, and temperature. What is needed for practical radio applications, however, is the total attenuation for a specified propagation path over which the pressure and temperature may vary.

Calculations have been made by others at some frequencies and ray angles for attenuation of radio waves through the entire atmosphere. Those of Bean and Abbott (3) are applicable to scatter-propagation links at the frequencies 100, 300, 3000, 10,000, 22,200, 32,500, and 50,000 megacycles, but are not directly applicable to radar calculations at ranges within the atmosphere. Hogg (4) has also calculated the absorption through the entire atmosphere at several elevation angles and at frequencies above 500 megacycles, but these results are also not applicable to radar targets inside the atmosphere.

To determine the attenuation starting with the Van Vleck equations for each specific case of radar range calculation would be excessively tedious. The objective of the present work has been to make calculations for ray paths at a number of elevation angles for typical atmospheric conditions, assuming one terminal of the path to be near the ground. The frequency range of interest is taken to be 100 to 10,000 megacycles. The results are presented in the form of curves from which the total attenuation may be read directly as a function of the total path length (range), for a number of elevation angles from zero to 10 degrees, and for a number of frequencies within the range of interest. The absorption at intermediate angles and frequencies may be estimated by interpolation.

The attenuation is given for the radar case of two-way transit of the specified path. However, the curves may be used also for one-way propagation by taking half the decibel values shown for the indicated range. These curves are presented as Figs. 1a to 1f. The text of this report describes the procedure by which these curves were obtained.

As workers in the microwave physics field are aware, there is some uncertainty* as to whether the Van Vleck-Weisskopf collision-broadening formula is exactly correct at frequencies far removed from resonance, and whether the pressure dependence of the line breadth is linear. Questions also exist concerning the correct values of the line-breadth constants for both oxygen and water vapor (6).

The seeming disregard of these uncertainties in publishing the calculations presented in this report is based on the following philosophy. That there is <u>some</u> attenuation of radio waves by the atmosphere is unquestioned. The radio or radar engineer is confronted with the choice of either assuming that the attenuation does not exist, or of making calculations based on the best information that is available. The present report is simply an attempt to do the latter.

*See Ref. 2, p. 431, for example, and also Ref. 5.

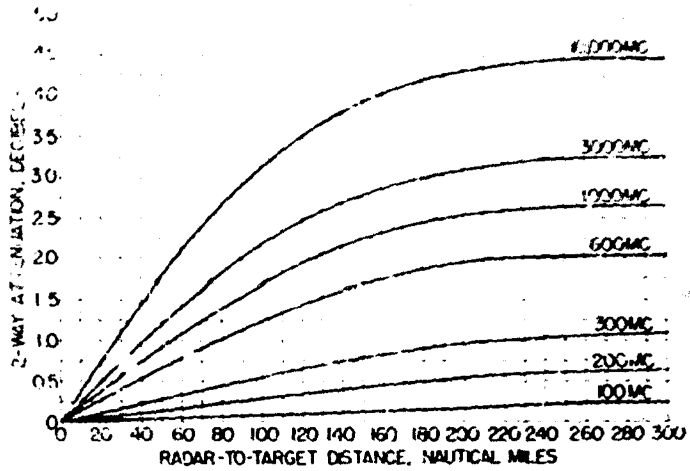

Fig. 1a - Radar atmospheric attenuation, 0° ray elevation angle

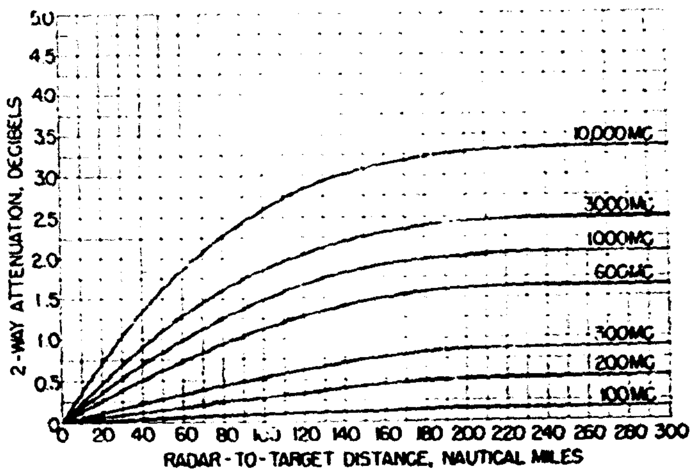

Fig. 1b - Radar atmospheric attenuation, 0.5° ray elevation angle

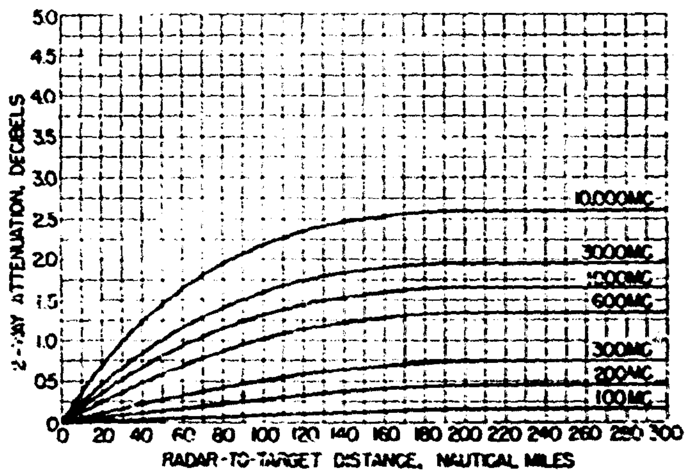

Fig. 1c - Radar atmospheric attenuation, 1.0° ray elevation angle

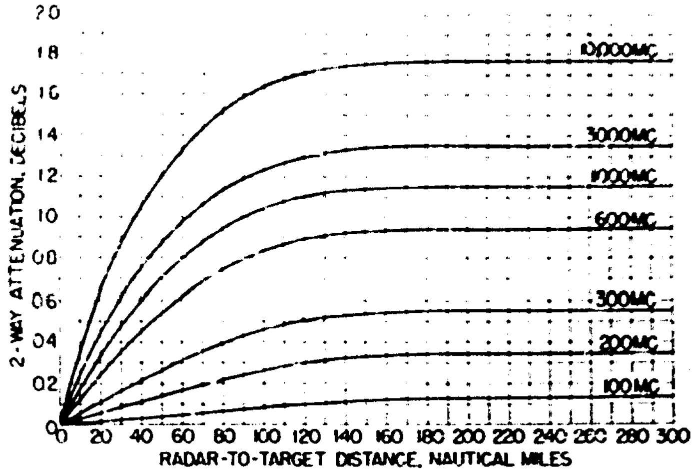

Fig. 1d - Radar atmospheric attenuation, 2.0° ray elevation angle

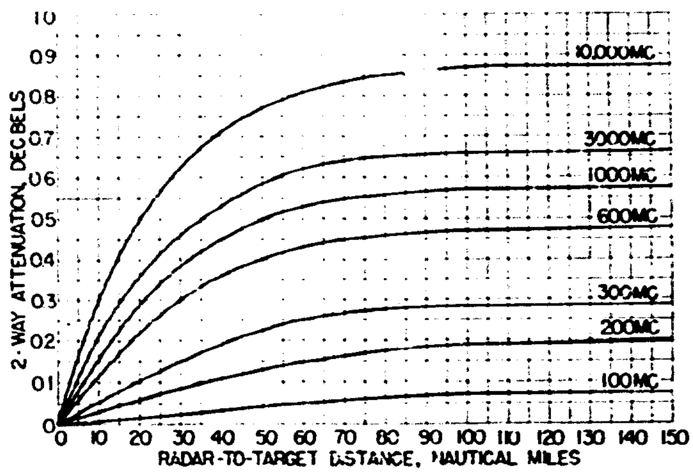

Fig. 1e - Radar atmospheric attenuation, 5.0° ray elevation angle

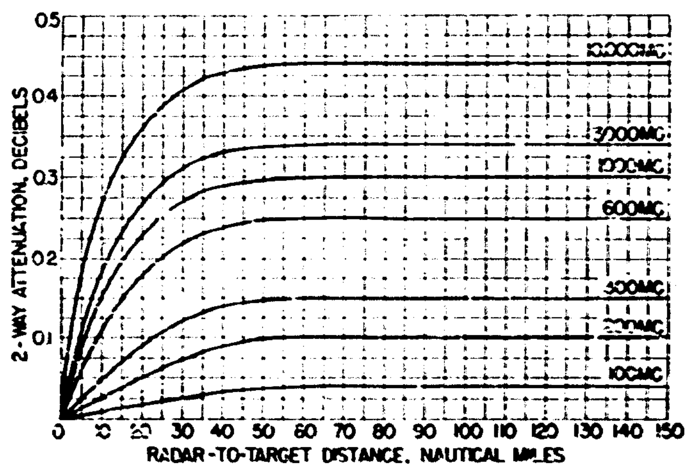

Fig. 1f - Radar atmospheric attenuation, 10° ray elevation angle

Some of the possible inaccuracies of the calculations are discussed in the report. Also, calculations of others in which similar assumptions are made are compared and, where comparable, the results are found to be in general agreement (3,4). It is believed that whatever criticism may be made on theoretical grounds, the curves presented herein are undoubtedly a better basis for making radar range calculations than has hitherto been generally available to the engineer. Also, they may serve as a model for the form in which improved information should be presented for engineering use.

The curves are calculated for a particular condition of the atmosphere, and hence do not apply exactly to all possible conditions. They are meant to be used for general radar range calculation, rather than for specific times and places, and for this purpose the adoption of a particular atmosphere as standard is of course necessary. The absorption values for other atmospheric conditions are, however, not greatly different, especially at the lower frequencies. Above 3000 megacycles, however, the variation in water-vapor content of the atmosphere may result in appreciable variation of the absorption.

The report of Bean and Abbott (3) provides an excellent indication of the variability to be expected. Below 1000 megacycles, the variation shown for widely different atmospheric conditions is of the order of 0.1 to 0.5 decibels, for a 300-mile scatter-propagation ray path. From 1000 to 10,000 megacycles the variation increases gradually to slightly more than one decibel. The range of atmospheric conditions considered was from those of Washington, D. C., in August to those of Bismarck, N. D., in February. No doubt a somewhat greater variability would be encountered for greater differences in geographic latitude.

The work reported here was performed in 1958-59, and was originally presented as a paper (7) at the URSI-IRE meetings in Washington, D. C., on May 6, 1959. The present report contains essentially the same information as the original paper except for additional notes and comments on the probable accuracy and applicability of the results, and comparison with results calculated by others.

The curves for radar attenuation by the atmosphere were also included in an NRL Memorandum Report (8), "Interim Report on Basic Pulse-Radar Maximum-Range Calculation," and will be included in a more complete report on this subject that is in preparation.

THE VAN VLECK THEORY

Absorption of radio waves in the normal atmosphere is due to the magnetic dipole moment of the oxygen molecule and the electric dipole moment of the water-vapor molecule. The resonance lines due to quantum-energy-state transitions are broadened by the effect of molecular collisions, so that even though the resonances are in the millimeter-wavelength region, some absorption occurs at frequencies far removed from resonance. In addition, the oxygen molecule has a nonresonant component of absorption.

Equation for Oxygen Absorption

The Van Vleck equation for oxygen in a form essentially the same as used by Bean and Abbott (3) is

$$\gamma_{O_2} = 28.809 \frac{p\nu^2}{T^2} \left\{ \frac{[1.704\, pT^{-1/2}\, (\Delta\nu)_1]}{\nu^2 + [1.704 \times 10^{-2}\, pT^{-1/2}\, (\Delta\nu)_1]^2} \right.$$

$$+ \frac{[1.704\, pT^{-1/2}\, (\Delta\nu)_2]}{(\nu_0 - \nu)^2 + [1.704 \times 10^{-2}\, pT^{-1/2}\, (\Delta\nu)_2]^2}$$

$$\left. + \frac{[1.704\, pT^{-1/2}\, (\Delta\nu)_2]}{(\nu_0 + \nu)^2 + [1.704 \times 10^{-12}\, pT^{-1/2}\, (\Delta\nu)_2]^2} \right\}. \qquad (1)$$

The symbols are defined as follows:

γ_{O_2} - oxygen absorption, decibels per kilometer

ν - wave number, cm^{-1} (reciprocal of wavelength, cm)*

ν_0 - resonance wave number for oxygen, 2 cm^{-1}

$(\Delta\nu)_1$ - line-breadth constant at sea level for nonresonant part of absorption, cm^{-1}

$(\Delta\nu)_2$ - line-breadth constant at sea level for resonant part of absorption, cm^{-1}

p - atmospheric pressure, millibars

T - atmospheric temperature, degrees Kelvin.

In Eq. (1), the temperature and pressure dependence of the line breadth is expressed by the terms in square brackets. Van Vleck mentions that the pressure dependence is subject to some uncertainty; it may not be quite linear. However, he deduces that the linear assumption is the best one to make until or unless experiments indicate a definite preference for another law.

The first term of the equation gives the nonresonant part of the absorption, while the second two give the resonance absorption. The second and third terms are the so-called structure factor of the collision-broadened resonance line at $\nu_0 = 2$ cm^{-1} ($f = 60{,}000$ megacycles). As Van Vleck points out, at frequencies near resonance, the second term predominates, and the third term is often omitted; however, it must be included when frequencies appreciably removed from resonance are to be considered, as they are here.

---

*The wave-number notation employed by spectroscopists sometimes causes confusion. In some of the literature the symbol ν is defined as the frequency. The line-breadth wave-number constants are then designated $\Delta\nu/c$, where c is the velocity of electromagnetic propagation, 3×10^{10} cm/sec. Here, however, the symbol ν denotes the wave number, to which the wavelength λ, and the frequency f are related as follows: $\nu = 1/\lambda = f/c$. Hence, $\Delta f = c\Delta\nu$.

The values to be used for $(\Delta\nu)_1$ and $(\Delta\nu)_2$ cannot readily be determined theoretically. Van Vleck concluded that the best choice on the basis of experiments was $\Delta\nu = 0.02\ cm^{-1}$. Bean and Abbott (3), on the basis of more recent experiments, adopted the values $(\Delta\nu)_1 = 0.018\ cm^{-1}$ and $(\Delta\nu)_2 = 0.05\ cm^{-1}$. These latter values have been used in the calculations made here. Subsequently, however, information from various sources has indicated that the value $\Delta\nu = 0.02\ cm^{-1}$ is probably still the best choice, and that no distinction should be made between $(\Delta\nu)_1$ and $(\Delta\nu)_2$. Fortunately, the calculated values of absorption in the frequency region of interest here depend primarily on the value chosen for $(\Delta\nu)_1$, so that the results given here do not differ appreciably from those that would be calculated for $\Delta\nu = 0.02\ cm^{-1}$. Moreover, the measurements on which the determination of $\Delta\nu$ is based are all subject to a considerable experimental error, so that there would not be much justification for revising the calculations. (That is, the results calculated here do not differ from those that would be calculated using $(\Delta\nu)_1 = (\Delta\nu)_2 = 0.02\ cm^{-1}$ by more than the experimental error that is inherent in using any value of $\Delta\nu$ that might be chosen on the basis of present knowledge.)

The dependence of the absorption on the values chosen for $(\Delta\nu)_1$ and $(\Delta\nu)_2$ is quite complicated, as inspection of the equation shows. The effect of using different values in the frequency range below 10,000 megacycles is best indicated by the following approximation, which is derived in Appendix A:

$$\gamma_{O_2} = 0.9091 \frac{p^2}{T^{5/2}} (\Delta\nu)_1 \left[\frac{1}{1 + 2.994 \times 10^{-4} \lambda^2 p^2 T^{-1} (\Delta\nu)_1^2} \right] \times \left[1 + \frac{0.5\ (\Delta\nu)_2}{\lambda^2\ (\Delta\nu)_1} \right] \qquad (2)$$

where λ is the wavelength in centimeters ($= 1/\nu$) and γ_{O_2} is the absorption in decibels per nautical mile. At $\lambda = 3$ cm (corresponding to f = 10,000 megacycles, the upper frequency limit of the range considered), the net effect of using the values $(\Delta\nu)_1 = 0.018$ and $(\Delta\nu)_2 = 0.05$ is about a 1-percent decrease in the value of γ_{O_2} at sea level, compared to using $(\Delta\nu)_1 = (\Delta\nu)_2 = 0.02$. At the lower frequency limit of 100 megacycles ($\lambda = 300$ cm), the only value that has appreciable effect is $(\Delta\nu)_1$. At sea level, the effect of using $(\Delta\nu)_1 = 0.018$ rather than 0.02 is to increase the value of γ_{O_2} about 10 percent at this frequency. At higher altitudes and higher frequencies the effect is smaller.

Equation (2) was used to calculate the oxygen absorption in the range 100 to 10,000 megacycles.

Equation for Water-Vapor Absorption

Compared to the oxygen attenuation, the absorption by the water-vapor content of the air is negligible below 3000 megacycles, and between 3000 and 10,000 megacycles its effect is minor though not negligible.

The equation for the water-vapor attenuation, as given by Bean and Abbott (3) is

$$\gamma_{H_2O} = 1.012 \times 10^{-3} \frac{\rho p \nu^2}{T} \left\{ \frac{[1.689 \times 10^{-2}\ pT^{-1/2}\ (\Delta\nu)_3]}{(\nu_1 - \nu)^2 + [1.689 \times 10^{-2}\ pT^{-1/2}\ (\Delta\nu)_3]^2} + \frac{[1.689 \times 10^{-2}\ pT^{-1/2}\ (\Delta\nu)_3]}{(\nu_1 + \nu)^2 + [1.689 \times 10^{-2} pT^{-1/2}\ (\Delta\nu)_3]^2} \right\}$$

$$+\ 3.471 \times 10^{-3} \frac{\rho p \nu^2}{T} [1.689 \times 10^{-2}\ pT^{-1/2}\ (\Delta\nu)_4] \qquad (3)$$

where the symbols that also appear in Eq. (1) have the same meanings; the additional symbols are defined as follows:

γ_{H_2O} - water-vapor absorption, decibels per kilometer

ρ - water-vapor density, grams per cubic meter

ν_1 - 0.742 cm^{-1}, wave number corresponding to the water-vapor resonance at λ = 1.35 cm (f = 22,200 megacycles)*

$(\Delta\nu)_3$ - line-breadth constant for the 22,200-megacycle resonance line

$(\Delta\nu)_4$ - an effective line-breadth constant for the aggregate effect of resonance lines above 22,200 megacycles.

The first two terms of this equation are for the resonance absorption at 22,200 megacycles (ν_1 = 0.742 cm^{-1}) while the third term is an approximation for the net effect of numerous higher frequency absorption lines.

The line-breadth constants $(\Delta\nu)_3$ and $(\Delta\nu)_4$ were estimated to have the value 0.1 cm^{-1}, by Van Vleck (2). On the basis of more recent measurements it has been concluded (4) that the composite effect of the higher frequency lines is better represented by using a value $(\Delta\nu)_4$ = 0.3 cm^{-1}. Straiton and Tolbert have discussed this matter (6) and conclude that additional measured values of water-vapor absorption in the millimeter wave region are higher than predicted by the Van Vleck-Weisskopf equation using either of these values of $(\Delta\nu)_4$. The general impression given is that reliable calculation of the water-vapor absorption is not possible at present.

Fortunately, as previously mentioned, the water-vapor absorption is insignificant below 3000 megacycles and is only relatively minor factor between 3000 and 10,000 megacycles. Therefore, while this component of the total atmospheric absorption should be taken into account, the exact values of the constants used in the water-vapor equation do not affect the total absorption significantly except at low elevation angles above 3000 megacycles.

The calculations resulting in the curves of this report are based on the values $(\Delta\nu)_3$ and $(\Delta\nu)_4$ equal to 0.1 cm^{-1}.

Equation (3) may be written in a more convenient form by collecting the common factors, inserting the value ν_1 = 0.742 cm^{-1}, writing $1/\lambda$ in place of ν, and multiplying by 1.852 to give the absorption in decibels per nautical mile:

$$\gamma_{H_2O} = 3.165 \times 10^{-6} \frac{\rho p^2}{T^{3/2}} \left[\frac{1}{(1 - 0.742\,\lambda)^2 + 2.853 \times 10^{-6}\,\lambda^2 p^2 T^{-1}} + \frac{1}{(1 + 0.742\,\lambda)^2 + 2.853 \times 10^{-6}\,\lambda^2 p^2 T^{-1}} + \frac{3.43}{\lambda^2} \right]. \tag{4}$$

*The best value for this resonance line, according to Van Vleck (2), is a measurement by Townes and Merritt giving the value λ = 1.3481 cm, from which ν = 0.7418.

OUTLINE OF CALCULATION PROCEDURE

Equations (2) and (4) were used to calculate the curves of Fig. 2, showing absorption in decibels per nautical mile as a function of altitude. The values of pressure, temperature, and water-vapor density used in this calculation are shown in Table 1. The pressure and temperature values are the ten-year averages prior to 1956 for April in Washington, D. C. The water-vapor values are the ten-year averages prior to 1945. These data were obtained from B. Ratner of the U.S. Weather Bureau.

Table 1
Atmosphere Characteristics Used for Absorption Calculations

Altitude (ft)	Pressure (millibars)	Temperature (°K)	Water-Vapor Density (g/m³)
0	1015	285.1	6.18
2,500	927	282.8	4.93
5,000	842	278.5	3.74
10,000	692	270.0	2.01
20,000	460	250.5	0.34
30,000	295	227.5	0.05
40,000	183	214.5	<0.01
60,000	68	213.0	-
80,000	26	220.5	-

Figure 2 gives the absorption per unit distance, γ, as a function of altitude, h. What is wanted is the total absorption, A, along a two-way ray path from the radar to the target and return. This total absorption is the integral of γ along the ray path. The geometry of the problem is shown by Fig. 3.

The first step in solving this problem is to obtain curves for γ as a function of the distance (or range), R, along a ray path of particular initial elevation angle, θ. This was done using values of altitude vs range calculated by J. R. Bauer et al. of the M.I.T. Lincoln Laboratory (9) for atmospheric characteristics approximately the same as those shown in Table 1.* The resulting curves are of the type of Figs. 4a and 4b. These curves were then integrated to obtain the values of attenuation, according to the formula

$$A(R_1;\theta,\lambda) = 2\int_0^{R_1} \gamma(R;\theta,\lambda)\, dR \tag{5}$$

where the factor 2 on the right-hand side accounts for the two-way traverse of the propagation path by radar signals.

The integration was performed numerically, using Simpson's rule, for each of six elevation angles and for each of seven frequencies. Since Simpson's rule requires only the ordinate values at regularly spaced intervals, it was not actually necessary to plot each of the 42 curves of the type of Figs. 4a and 4b. The final results are plotted in Figs. 1a to 1f. Appendix B contains tabulations of the computed values for the various steps of the calculations, as well as the final results from which Fig. 1 is plotted. Application of these results to radar range calculation is discussed in Appendix C.

*Additional discussion of the radio-ray range-height-angle relationship is contained in Ref. 10.

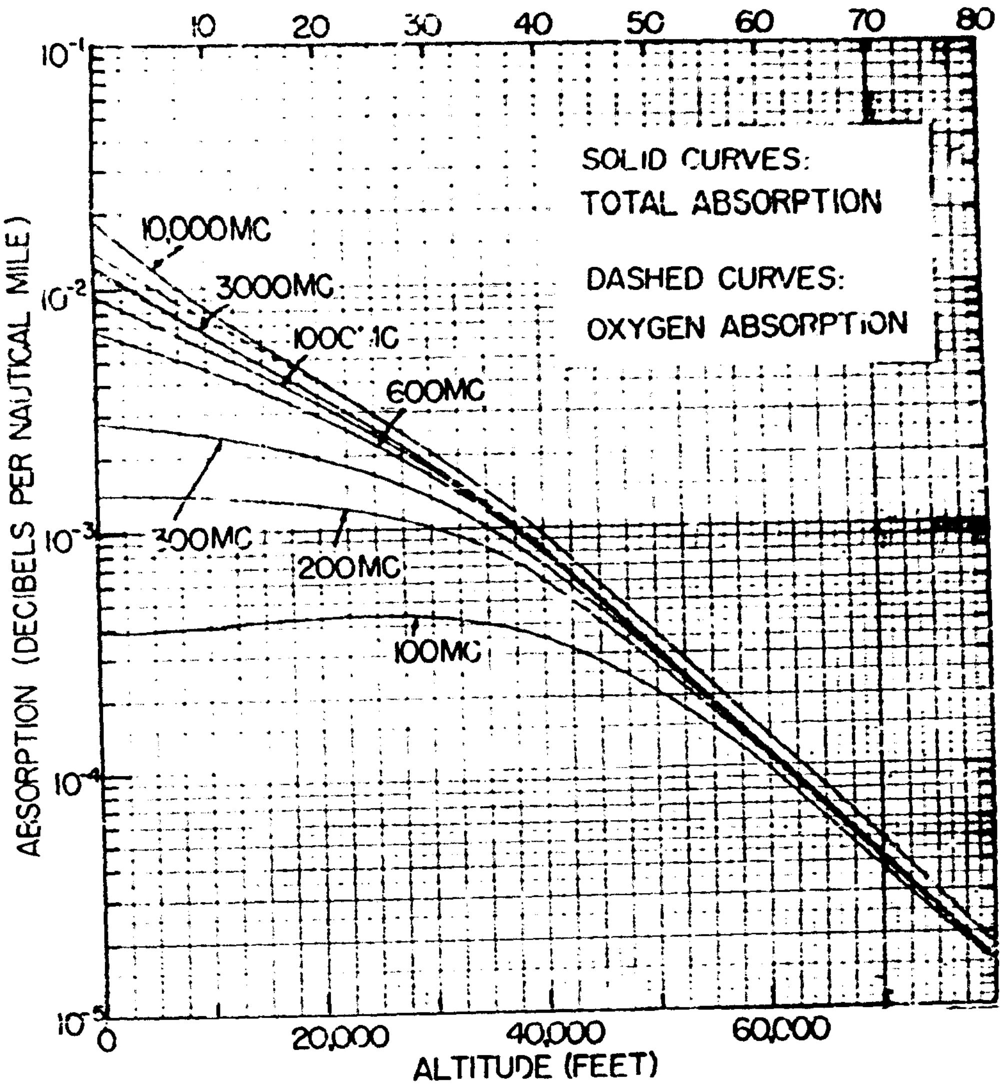

Fig. 2 - Absorption as a function of altitude and radio frequency for a temperate-zone cool atmosphere

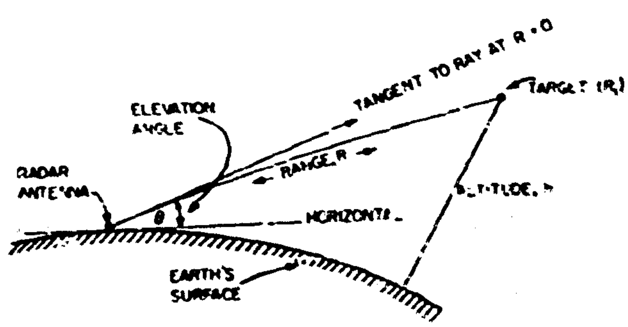

Fig. 3 - Geometry of propagation-path aspect of attenuation calculation

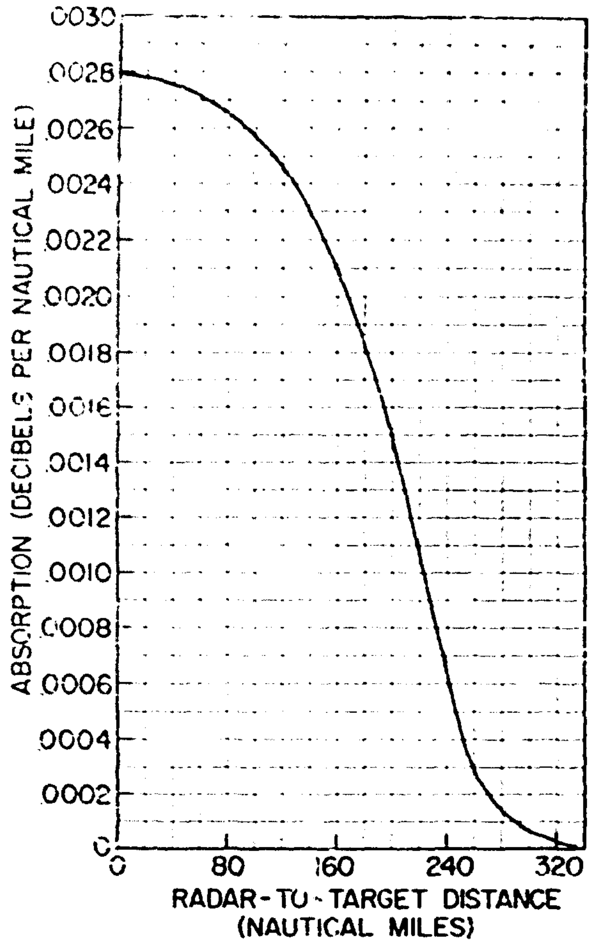

Fig. 4a - Attenuation rate as a function of distance along ray path of 0° elevation angle for 300 Mc

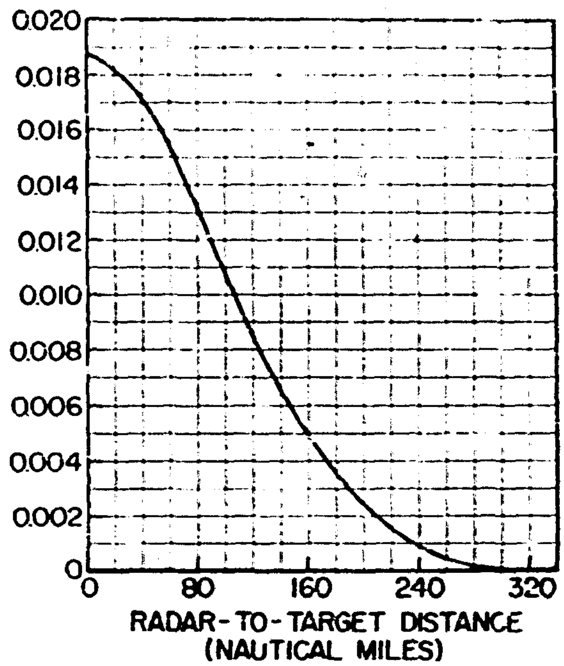

Fig. 4b - Attenuation rate as a function of distance along ray path of 0° elevation angle for 10,000 Mc

DISCUSSION OF RESULTS

At the frequencies and elevation angles where comparison is possible, the results calculated here are in general agreement with those calculated by Bean and Abbott (3) for two-way transmission through the entire atmosphere, and by Hogg (4) for one-way transmission through the entire atmosphere. Hogg's absorption figures are somewhat higher than those reported here, increasingly so as the frequency is increased. Presumably, this is due primarily to the differences in values of the constants used in calculating the water-vapor absorption. As Table 1 indicates, the value of water-vapor density at sea level was assumed to be 6.18 grams per cubic meter, while Hogg assumed a value of 10 grams per cubic meter. Also, Hogg used the value $(\Delta\nu)_4 = 0.3$ whereas here the value $(\Delta\nu)_4 = 0.1$ was used. Both of these differences would cause Hogg's values to be somewhat higher than those calculated here.

A possible further factor is Hogg's assumption of a linear decay of water-vapor density with altitude, while here a more nearly exponential decay was assumed. Also, Hogg assumed a ray path based on linear decay of the refractive index with altitude (the "4/3-earth's curvature" model), whereas here Bauer's negative-exponential model of refractive index decay (9) was assumed. The former model results in a lower-altitude path for a given initial ray angle, hence slightly greater absorption.

As mentioned previously, the choice of $(\Delta\nu)_4 = 0.3$, used by Hogg, is probably preferable to the value $(\Delta\nu)_4 = 0.1$ as used here, but the theoretical and experimental basis for this was not deemed sufficiently firm to justify revising the calculations.

The sea-level value of ρ, the water-vapor density, is an extremely variable quantity, ranging from less than 3 to above 20 grams per cubic meter (3), depending upon the season and locality. Therefore, the appropriate value to use for a purpose such as the present one is a value arbitrarily accepted as standard. There is apparently some agreement (6) on the value 7.5 grams per cubic meter as a standard. However, this differs so slightly from the value 6.18 used here (considering the relatively minor role of the water-vapor absorption at frequencies below 10,000 megacycles) that recalculation using this value was not deemed to be worthwhile.

The somewhat surprising thing about the values calculated is the appreciable absorption at frequencies of the order at 3000 megacycles and below, at low angles. Until rather recently it has been customary to assume that atmospheric absorption is negligible at these frequencies. The stimulus for making the present calculations, on which work was begun several years ago, was primarily the thought that the greater range of modern radars might make the absorption significant. But, as Fig. 1a shows, the absorption is significant even at moderate ranges, because the greater part of the loss occurs in the part of the ray path lying in the relatively dense lower atmosphere. The loss does not increase very greatly with range after the first 200 miles; in fact, about 50 to 70 percent of it (depending on the frequency) occurs in the first 100 miles. There is practically no additional absorption when the ray path is above 60,000 feet.

Even at 300 megacycles the loss is as much as a decibel at zero elevation and about 200-mile range, a not-insignificant amount. Admittedly, the accuracy of the calculated absorption at these low frequencies is questionable, but it seems preferable to use these calculated values in making radar range calculations than to assume that there is no absorption.

ACKNOWLEDGMENTS

The work reported here was greatly facilitated by the paper (3) of B. R. Bean and R. Abbott of the National Bureau of Standards, Boulder Laboratories, and by correspondence with them. Thanks are extended to John Gibson of the Naval Research Laboratory for helpful discussions and for mentioning the existence of the paper by Bean and Abbott. The competent assistance of Frank D. Clarke in performing the laborious computations is gratefully acknowledged.

REFERENCES

1. Van Vleck, J.H., "The Absorption of Microwaves by Oxygen," Phys. Rev. 71:413 (1947)

2. Van Vleck, J.H., "The Absorption of Microwaves by Uncondensed Water Vapor," Phys. Rev. 71:425 (1947)

3. Bean, B.R., and Abbott, R., "Oxygen and Water-Vapor Absorption of Radio Waves in the Atmosphere," Review Geofisica Pura E Applicata (Milano) 37:127 (1957)

4. Hogg, D.C., "Effective Antenna Temperatures Due to Oxygen and Water Vapor in the Atmosphere," J. Appl. Phys. 30:1417 (1959)

5. Van Vleck, J.H., and Weisskopf, V.F., "On the Shape of Collision-Broadened Lines," Rev. Mod. Phys. 17:227 (1945)

6. Straiton, A.W., and Tolbert, C.W., "Anomalies in the Absorption of Radio Waves by Atmospheric Gases," Proc. I.R.E. 48:898 (1960)

7. Blake, L.V., "Radar Attenuation by Atmospheric Oxygen," Paper presented at URSI-IRE Meeting of May 6, 1959, Commission 2: Tropospheric Radio Propagation (Washington, D.C.)

8. Blake, L.V., "Interim Report on Basic Pulse-Radar Maximum-Range Calculation," NRL Memorandum Report 1106, Nov. 1960

9. Bauer, J.R., Mason, W.C., Wilson, F.A., "Radio Refraction in a Cool Exponential Atmosphere," M.I.T. Lincoln Laboratory Technical Report 186, Aug. 27, 1958

10. Bean, B.R., and Thayer, G.D., "Models of the Atmospheric Radio Refractive Index," Proc. I.R.E. 47:740 (1959)

* * *

APPENDIX A

DERIVATION OF AN APPROXIMATION FOR THE ABSORPTION BY OXYGEN

The approximation to be derived is based on Eq. (1), and is for use at frequencies below 10,000 megacycles. Equation (1) may be written in the following form, by combining the numerical constants and the pressure-temperature terms in the numerators, by using the reciprocal of wavelength $(1/\lambda)$ in place of the wave number, and by taking $\nu_0 = 2\ \text{cm}^{-1}$ (no approximation is involved thus far):

$$\gamma_{O_2} = 0.4909 \frac{p^2}{\lambda^2 T^{5/2}} \left[\frac{(\Delta\nu)_1}{1/\lambda^2 + A^2 (\Delta\nu)_1^2} + \frac{(\Delta\nu)_2}{(2 - 1/\lambda)^2 + A^2 (\Delta\nu)_2^2} + \frac{(\Delta\nu)_2}{(2 + 1/\lambda)^2 + A^2 (\Delta\nu)_2^2} \right]$$

where $A = 1.704 \times 10^{-2}\ pT^{-1/2}$. Since $A \approx 1$ at sea-level temperature and pressure, and is otherwise less than one, and since $(\Delta\nu)_2^2$ is 0.0025 for $(\Delta\nu)_2 = 0.05$, then $A^2 (\Delta\nu)_2^2$ is of negligible magnitude compared to $(2 \pm 1/\lambda^2)$ for all values of $\lambda \geq 3$ cm. Therefore, the term $A^2 (\Delta\nu)_2^2$ may be dropped from the denominators of the second two terms of the equation. The entire expression may then be rewritten as follows:

$$\gamma_{c_2} = 0.4909 \frac{p^2}{\lambda^2 T^{5/2}} \left[\frac{(\Delta\nu)_1}{1/\lambda^2 + A^2 (\Delta\nu)_1^2} \right] \times \left\{ 1 + \frac{(\Delta\nu)_2}{(\Delta\nu)_1} \left[1/\lambda^2 + A^2 (\Delta\nu)_1^2 \right] \left[\frac{1}{(2 - 1\lambda)^2} + \frac{1}{(2 + 1/\lambda)^2} \right] \right\}.$$

The quantity

$$\left[\frac{1}{(2 - 1/\lambda)^2} + \frac{1}{(2 + 1/\lambda)^2} \right]$$

may be written

$$\left[\frac{2(4 + 1/\lambda^2)}{(4 - 1/\lambda^2)^2} \right].$$

If the approximation $(4 \pm 1/\lambda^2) \cong 4$ is made this expression is equal to 1/2, with a maximum error of about 5 percent, at $\lambda = 3$ cm. This results in a maximum error in the value of γ_{O_2} of only about 0.5 percent at $\lambda = 3$ cm. Also, the term $A^2 (\Delta\nu_1)^2/2$ is negligible compared to 1 and may be omitted. The resulting expression is

$$\gamma_{O_2} = 0.4909 \frac{p^2}{\lambda^2 T^{5/2}} \left[\frac{(\Delta\nu)_1}{1/\lambda^2 + A^2 (\Delta\nu)_1^2} \right] \times \left[1 + \frac{(\Delta\nu)_2 / (\Delta\nu)_1}{2\lambda^2} \right] \text{decibels per kilometer}$$

or

$$\gamma_{O_2} = 0.909 \frac{p^2}{T^{5/2}} \left[\frac{(\Delta\nu)_1}{1 + 2.904 \times 10^{-4} p^2 \lambda^2 T^{-1} (\Delta\nu)_1^2} \right] \left[1 + \frac{(\Delta\nu)_2 / (\Delta\nu)_1}{2\lambda^2} \right] \text{decibels per nautical mile.}$$

This is Eq. (2), which may be used to calculate γ_{O_2} with negligible difference from Eq. (1) in the frequency range below 10,000 megacycles.

* * *

APPENDIX B

SOME DETAILS AND NUMERICAL RESULTS OF THE CALCULATIONS

The approximation formula for oxygen absorption, Eq. (2), gives the following results at the particular altitudes for which pressure and temperature are given in Table 1. Writing the equation in the form

$$\gamma_{O_2} = P\left(\frac{1}{1 + Q\,\lambda^2}\right)\left(1 + \frac{1.39}{\lambda^2}\right)$$

the results are:

Altitude (feet)	P	Q
0	1.227×10^{-2}	3.398×10^{-4}
2,500	1.045×10^{-2}	2.858×10^{-4}
5,000	8.964×10^{-3}	2.395×10^{-4}
10,000	6.539×10^{-3}	1.669×10^{-4}
20,000	3.485×10^{-3}	7.945×10^{-5}
30,000	1.824×10^{-3}	3.599×10^{-5}
40,000	8.129×10^{-4}	1.468×10^{-5}
60,000	1.143×10^{-4}	2.042×10^{-6}
80,000	1.532×10^{-5}	2.884×10^{-7}

Quantities occurring in the water-vapor absorption equation, Eq. (4), have the following values at these altitudes:

Altitude (feet)*	3.165×10^{-6} $\times(\rho p^2/T^{3/2})$	2.853×10^{-8} $\times\, p^2T^{-1}$
0	4.184×10^{-3}	1.031×10^{-2}
2,500	2.818×10^{-3}	8.671×10^{-3}
5,000	1.804×10^{-3}	7.264×10^{-3}
10,000	6.871×10^{-4}	5.062×10^{-3}
20,000	5.744×10^{-5}	2.410×10^{-3}

*As will be seen on the next page, values above 20,000 feet result in negligible water-vapor absorption.

These results lead to the values of γ_{O_2} and γ_{H_2O} listed in the two tables that follow:

Altitude (feet)	Oxygen Absorption, γ_{O_2} (decibels per nautical mile)						
	100 Mc	200 Mc	300 Mc	600 Mc	1000 Mc	3000 Mc	10,000 Mc
0	3.93×10^{-4}	1.42×10^{-3}	2.79×10^{-3}	6.64×10^{-3}	9.40×10^{-3}	1.20×10^{-2}	1.41×10^{-2}
2,500	3.87×10^{-4}	1.41×10^{-3}	2.71×10^{-3}	6.11×10^{-3}	8.31×10^{-3}	1.04×10^{-2}	1.20×10^{-2}
5,000	3.94×10^{-4}	1.40×10^{-3}	2.64×10^{-3}	5.60×10^{-3}	7.37×10^{-3}	8.88×10^{-3}	1.03×10^{-2}
10,000	4.05×10^{-4}	1.38×10^{-3}	2.45×10^{-3}	4.60×10^{-3}	5.69×10^{-3}	6.52×10^{-3}	7.53×10^{-3}
20,000	4.29×10^{-4}	1.25×10^{-3}	1.94×10^{-3}	2.90×10^{-3}	3.25×10^{-3}	3.51×10^{-3}	4.02×10^{-3}
30,000	4.30×10^{-4}	1.01×10^{-3}	1.34×10^{-3}	1.67×10^{-3}	1.77×10^{-3}	1.84×10^{-3}	2.11×10^{-3}
40,000	3.50×10^{-4}	6.11×10^{-4}	7.09×10^{-4}	7.34×10^{-3}	8.02×10^{-4}	8.23×10^{-4}	9.38×10^{-4}
60,000	9.68×10^{-5}	1.09×10^{-4}	1.12×10^{-4}	1.14×10^{-4}	1.14×10^{-4}	1.16×10^{-4}	1.32×10^{-4}
80,000	1.49×10^{-5}	1.52×10^{-5}	1.53×10^{-5}	1.53×10^{-5}	1.53×10^{-5}	1.53×10^{-5}	1.77×10^{-5}

Altitude (feet)	Water-Vapor Absorption, γ_{H_2O} (decibels per nautical mile)			
	<1000 Mc	1000 Mc	3000 Mc	10,000 Mc
0		3.3×10^{-5}	3.01×10^{-4}	4.62×10^{-3}
2,500	negligible	negligible	2.03×10^{-4}	3.16×10^{-3}
5,000			1.30×10^{-4}	2.06×10^{-3}
10,000			4.95×10^{-5}	7.76×10^{-4}
20,000			4.14×10^{-6}	6.55×10^{-5}
>20,000			negligible	negligible

The values for γ used to plot Fig. 2 are obtained by adding the values in the preceding two tables.

The values of ordinates of the $\gamma(R;\theta,\lambda)$ curves, of the type of Fig. 4, are given in the following table:

Range (naut mi)	Alt. (feet)	Attenuation (db per nautical mile)						
		100 Mc	200 Mc	300 Mc	600 Mc	1000 Mc	3000 Mc	10,000 Mc
Zero-Degree Ray								
0	0	3.93×10^{-4}	1.42×10^{-3}	2.79×10^{-3}	6.64×10^{-3}	9.40×10^{-3}	1.23×10^{-2}	1.87×10^{-2}
20	346	3.92×10^{-4}	1.42×10^{-3}	2.78×10^{-3}	6.60×10^{-3}	9.20×10^{-3}	1.21×10^{-2}	1.82×10^{-2}
40	1,147	3.90×10^{-4}	1.42×10^{-3}	2.75×10^{-3}	6.40×10^{-3}	8.90×10^{-3}	1.16×10^{-2}	1.70×10^{-2}
60	2,486	3.87×10^{-4}	1.41×10^{-3}	2.71×10^{-3}	6.11×10^{-3}	8.31×10^{-3}	1.06×10^{-2}	1.52×10^{-2}
80	4,373	3.90×10^{-4}	1.40×10^{-3}	2.65×10^{-3}	5.70×10^{-3}	7.60×10^{-3}	9.40×10^{-3}	1.31×10^{-2}
100	6,817	3.98×10^{-4}	1.40×10^{-3}	2.57×10^{-3}	5.20×10^{-3}	6.60×10^{-3}	8.00×10^{-3}	1.07×10^{-2}
120	9,832	4.07×10^{-4}	1.38×10^{-3}	2.46×10^{-3}	4.60×10^{-3}	5.70×10^{-3}	6.62×10^{-3}	8.40×10^{-3}
160	17,629	4.29×10^{-4}	1.29×10^{-3}	2.08×10^{-3}	3.25×10^{-3}	3.75×10^{-3}	4.05×10^{-3}	4.88×10^{-3}
200	27,882	4.39×10^{-4}	1.07×10^{-3}	1.49×10^{-3}	1.90×10^{-3}	2.03×10^{-3}	2.13×10^{-3}	2.40×10 [illegible]
250	44,320	2.89×10^{-4}	4.29×10^{-4}	4.30×10^{-4}	4.87×10^{-4}	5.30×10^{-4}	5.41×10^{-4}	6.20×10^{-4}
300	64,932	6.00×10^{-5}	6.65×10^{-5}	6.90×10^{-5}	7.00×10^{-5}	7.00×10^{-5}	7.00×10^{-5}	8.15×10^{-5}
330	79,348	1.58×10^{-5}	1.63×10^{-5}	1.64×10^{-5}	1.65×10^{-5}	1.65×10^{-5}	1.67×10^{-5}	1.9×10^{-5}
0.5-Degree Ray								
0	0	3.93×10^{-4}	1.42×10^{-3}	2.79×10^{-3}	6.64×10^{-3}	9.40×10^{-3}	1.23×10^{-2}	1.87×10^{-2}
20	1,408	3.89×10^{-4}	1.42×10^{-3}	2.73×10^{-3}	6.35×10^{-3}	8.70×10^{-3}	1.13×10^{-2}	1.67×10^{-2}
40	3,276	3.89×10^{-4}	1.41×10^{-3}	2.70×10^{-3}	5.95×10^{-3}	7.99×10^{-3}	1.00×10^{-2}	1.43×10^{-2}
60	5,695	3.95×10^{-4}	1.40×10^{-3}	2.60×10^{-3}	5.45×10^{-3}	7.00×10^{-3}	8.60×10^{-3}	1.17×10^{-2}
80	8,680	4.00×10^{-4}	1.38×10^{-3}	2.50×10^{-3}	4.82×10^{-3}	6.05×10^{-3}	7.16×10^{-3}	9.30×10^{-3}
100	12,243	4.15×10^{-4}	1.36×10^{-3}	2.35×10^{-3}	4.16×10^{-3}	5.02×10^{-3}	5.70×10^{-3}	7.10×10^{-3}
120	16,401	4.27×10^{-4}	1.30×10^{-3}	2.13×10^{-3}	3.43×10^{-3}	4.00×10^{-3}	4.37×10^{-3}	5.30×10^{-3}
160	26,562	4.40×10^{-4}	1.11×10^{-3}	1.57×10^{-3}	2.05×10^{-3}	2.20×10^{-3}	2.33×10^{-3}	2.65×10^{-3}
200	39,278	3.60×10^{-4}	6.40×10^{-4}	7.50×10^{-4}	8.45×10^{-4}	8.60×10^{-4}	8.90×10^{-4}	1.00×10^{-3}
250	58,903	1.06×10^{-4}	1.20×10^{-4}	1.24×10^{-4}	1.26×10^{-4}	1.26×10^{-4}	1.28×10^{-4}	1.47×10^{-4}
300	82,783	1.11×10^{-5}	1.20×10^{-5}	1.20×10^{-5}	1.20×10^{-5}	1.20×10^{-5}	1.20×10^{-5}	1.40×10^{-5}

Range (naut mi)	Alt. (feet)	Attenuation (db per nautical mile)						
		100 Mc	200 Mc	300 Mc	600 Mc	[illegible] Mc	3000 Mc	10,000 Mc
1-Degree Ray								
0	0	3.93×10^{-4}	1.42×10^{-3}	2.79×10^{-3}	6.64×10^{-3}	9.40×10^{-3}	1.23×10^{-2}	1.87×10^{-2}
20	2,470	3.88×10^{-4}	1.41×10^{-3}	2.70×10^{-3}	6.10×10^{-3}	8.30×10^{-3}	1.06×10^{-2}	1.53×10^{-2}
40	5,405	3.95×10^{-4}	1.40×10^{-3}	2.61×10^{-3}	5.50×10^{-3}	7.15×10^{-3}	8.78×10^{-3}	1.20×10^{-2}
60	8,901	4.03×10^{-4}	1.38×10^{-3}	2.50×10^{-3}	4.80×10^{-3}	[illegible]	7.03×10^{-3}	9.00×10^{-3}
80	12,982	[illegible]	1.35×10^{-3}	2.30×10^{-3}	4.00×10^{-3}	4.80×10^{-3}	5.41×10^{-3}	6.70×10^{-3}
100	17,652	4.29×10^{-4}	1.29×10^{-3}	2.08×10^{-3}	3.25×10^{-3}	3.73×10^{-3}	4.05×10^{-3}	4.90×10^{-3}
120	22,942	4.39×10^{-4}	1.19×10^{-3}	1.79×10^{-3}	2.50×10^{-3}	2.71×10^{-3}	2.93×10^{-3}	3.39×10^{-3}
160	35,412	4.00×10^{-4}	8.20×10^{-4}	9.81×10^{-4}	1.15×10^{-3}	1.18×10^{-3}	1.22×10^{-3}	[illegible]
200	50,502	2.00×10^{-4}	2.55×10^{-4}	2.79×10^{-4}	2.85×10^{-4}	2.88×10^{-4}	2.95×10^{-4}	3.40×10^{-4}
240	68,292	4.41×10^{-5}	4.82×10^{-5}	5.00×10^{-5}	5.05×10^{-5}	5.05×10^{-5}	5.05×10^{-5}	5.85×10^{-5}
2-Degree Ray								
0	0	3.93×10^{-4}	1.42×10^{-3}	2.79×10^{-3}	6.64×10^{-3}	9.40×10^{-3}	1.23×10^{-2}	1.87×10^{-2}
20	4,590	3.90×10^{-4}	1.41×10^{-3}	2.65×10^{-3}	5.66×10^{-3}	7.40×10^{-3}	9.30×10^{-3}	1.29×10^{-2}
40	9,658	4.05×10^{-4}	1.38×10^{-3}	2.46×10^{-3}	4.65×10^{-3}	5.75×10^{-3}	6.70×10^{-3}	8.50×10^{-3}
60	15,312	4.24×10^{-4}	1.32×10^{-3}	2.19×10^{-3}	3.60×10^{-3}	4.25×10^{-3}	4.68×10^{-3}	5.70×10^{-3}
80	21,562	4.38×10^{-4}	1.22×10^{-3}	1.67×10^{-3}	2.70×10^{-3}	2.97×10^{-3}	3.22×10^{-3}	3.73×10^{-3}
100	28,442	4.38×10^{-4}	1.06×10^{-3}	1.45×10^{-3}	1.83×10^{-3}	1.96×10^{-3}	2.05×10^{-3}	[illegible]
120	35,962	3.95×10^{-4}	8.00×10^{-4}	9.50×10^{-4}	1.10×10^{-3}	1.13×10^{-3}	1.18×10^{-3}	1.32×10^{-3}
160	53,982	1.57×10^{-4}	1.87×10^{-4}	2.00×10^{-4}	2.05×10^{-4}	2.06×10^{-4}	2.15×10^{-4}	2.46×10^{-4}
200	72,692	2.90×10^{-5}	3.10×10^{-5}	3.20×10^{-5}	3.20×10^{-5}	3.20×10^{-5}	3.20×10^{-5}	3.70×10^{-5}

Range (naut mi)	Alt. (feet)	Attenuation (db per nautical mile)						
		100 Mc	200 Mc	300 Mc	600 Mc	1000 Mc	3000 Mc	10,000 Mc
5-Degree Ray								
0	0	3.93×10^{-4}	1.42×10^{-3}	2.79×10^{-3}	6.64×10^{-3}	9.40×10^{-3}	1.23×10^{-2}	1.87×10^{-2}
10	5,442	3.94×10^{-4}	1.40×10^{-3}	2.61×10^{-3}	5.50×10^{-3}	7.13×10^{-3}	8.75×10^{-3}	1.20×10^{-2}
20	10,942	4.10×10^{-4}	1.36×10^{-3}	2.40×10^{-3}	4.40×10^{-3}	5.37×10^{-3}	6.15×10^{-3}	7.75×10^{-3}
30	16,592	4.27×10^{-4}	1.30×10^{-3}	2.13×10^{-3}	3.41×10^{-3}	4.00×10^{-3}	4.35×10^{-3}	5.25×10^{-3}
40	22,392	4.40×10^{-4}	1.20×10^{-3}	1.81×10^{-3}	2.57×10^{-3}	2.80×10^{-3}	3.01×10^{-3}	3.50×10^{-3}
50	28,342	4.39×10^{-4}	1.07×10^{-3}	1.46×10^{-3}	1.85×10^{-3}	1.99×10^{-3}	2.08×10^{-3}	2.33×10^{-3}
60	34,462	4.10×10^{-4}	8.60×10^{-4}	1.05×10^{-3}	1.23×10^{-3}	1.27×10^{-3}	1.32×10^{-3}	1.48×10^{-3}
80	47,172	2.48×10^{-4}	3.40×10^{-4}	3.80×10^{-4}	3.98×10^{-4}	4.00×10^{-4}	4.10×10^{-4}	4.70×10^{-4}
100	60,562	9.20×10^{-5}	1.03×10^{-4}	1.06×10^{-4}	1.08×10^{-4}	1.10×10^{-4}	1.10×10^{-4}	1.26×10^{-4}
120	74,612	2.45×10^{-5}	2.60×10^{-5}	2.65×10^{-5}	2.65×10^{-5}	2.65×10^{-5}	2.65×10^{-5}	3.10×10^{-5}
10-Degree Ray								
0	0	3.93×10^{-4}	1.42×10^{-3}	2.79×10^{-3}	6.64×10^{-3}	9.40×10^{-3}	1.23×10^{-2}	1.87×10^{-2}
10	10,700	4.10×10^{-4}	1.37×10^{-3}	2.42×10^{-3}	4.43×10^{-3}	5.45×10^{-3}	6.25×10^{-3}	7.90×10^{-3}
20	21,450	4.40×10^{-4}	1.18×10^{-3}	1.74×10^{-3}	2.38×10^{-3}	2.57×10^{-3}	2.76×10^{-3}	3.15×10^{-3}
30	32,360	4.20×10^{-4}	9.40×10^{-4}	1.19×10^{-3}	1.42×10^{-3}	1.48×10^{-3}	1.54×10^{-3}	1.73×10^{-3}
40	43,430	3.05×10^{-4}	4.60×10^{-4}	5.25×10^{-4}	5.65×10^{-4}	5.75×10^{-4}	5.90×10^{-4}	6.70×10^{-4}
60	66,050	5.48×10^{-5}	6.00×10^{-5}	6.20×10^{-5}	6.25×10^{-5}	6.25×10^{-5}	6.30×10^{-5}	7.30×10^{-5}
80	89,340	5.60×10^{-6}	5.95×10^{-6}	6.20×10^{-6}	6.20×10^{-6}	6.20×10^{-6}	6.20×10^{-6}	7.20×10^{-6}
30-Degree Ray								
0	0	3.93×10^{-4}	1.42×10^{-3}	2.79×10^{-3}	6.64×10^{-3}	9.40×10^{-3}	1.23×10^{-2}	1.87×10^{-2}
5	15,230	4.22×10^{-4}	1.32×10^{-3}	2.20×10^{-3}	3.62×10^{-3}	4.28×10^{-3}	4.72×10^{-3}	5.77×10^{-3}
10	30,512	4.30×10^{-4}	1.00×10^{-3}	1.31×10^{-3}	1.61×10^{-3}	1.70×10^{-3}	1.77×10^{-3}	2×10^{-3}
20	61,062	8.8×10^{-5}	9.9×10^{-5}	1.00×10^{-4}	1.02×10^{-4}	1.02×10^{-4}	1.03×10^{-4}	1.2×10^{-4}
30	91,742	4.5×10^{-6}	4.5×10^{-6}	4.5×10^{-6}	4.8×10^{-6}	4.8×10^{-6}	4.8×10^{-6}	5.5×10^{-6}

The values obtained by Simpson's Rule integration of the γ (R:θ,λ) functions, using the ordinate values in the preceding tables, are as follows (these are the values used in plotting Figs. 1):

Range (naut mi)	Two-Way Attenuation (decibels)						
	100 Mc	200 Mc	300 Mc	600 Mc	1000 Mc	3000 Mc	10,000 Mc
Zero-Degree Ray							
20	-	-	-	-	-	-	0.74
40	0.03	0.11	0.22	0.53	0.73	0.96	1.45
60	-	-	-	-	-	-	2.09
80	0.06	0.23	0.44	1.01	1.40	1.81	2.36
100	-	-	-	-	-	-	3.13
120	0.09	0.34	0.64	1.43	.93	2.45	-
140	-	-	-	-	-	-	3.81
200	0.16	0.54	0.97	1.95	2.53	3.10	4.32
300	0.22	0.63	1.08	2.04	2.67	3.26	4.49
0.5-Degree Ray							
40	0.031	0.11	0.22	0.51	0.70	0.90	1.33
80	0.063	0.23	0.43	0.94	1.26	1.59	2.27
120	0.096	0.33	0.61	1.27	1.66	2.05	2.84
200	0.16	0.50	0.86	1.61	2.02	2.44	3.29
300	0.17	0.54	0.90	1.65	2.07	2.48	3.35
1.0-Degree Ray							
40	0.03	0.11	0.22	0.49	0.66	0.85	1.23
80	0.06	0.22	0.41	0.87	1.14	1.41	1.95
120	0.10	0.33	0.58	1.13	1.44	1.74	2.35
200	0.16	0.45	0.74	1.33	1.65	1.95	2.60
250	0.17	0.46	0.75	-	-	-	2.61
300	-	-	-	-	1.66	-	-
2-Degree Ray							
40	0.031	0.11	0.21	0.45	0.60	0.75	1.05
80	0.065	0.22	0.39	0.74	0.94	1.13	1.52
120	0.100	0.30	0.50	0.89	1.10	1.30	1.71
200	0.128	0.34	0.55	0.94	[illegible]	1.35	1.77

(Table Continues)

Table (continued)

Range (naut mi)	Two-Way Attenuation (decibels)						
	100 Mc	200 Mc	300 Mc	600 Mc	1000 Mc	3000 Mc	10,000 Mc
	5-Degree Ray						
20	0.016	0.06	0.10	0.22	0.29	0.36	0.50
40	0.033	0.11	0.19	0.36	0.45	0.53	0.71
60	0.050	0.15	0.25	0.43	0.53	0.62	0.81
100	0.070	0.19	0.283	0.47	0.57	0.659	0.87
110	0.073	0.193	0.286	0.473	0.573	0.662	0.873
	10-Degree Ray						
20	0.016	0.05	0.09	0.18	0.23	0.27	0.36
40	0.033	0.09	0.14	0.24	0.29	0.33	0.43
80	0.040	0.10	0.15	0.25	0.30	0.34	0.44

* * *

APPENDIX C

APPLICATION TO RADAR RANGE CALCULATION

The monostatic single-antenna radar equation written in terms of received signal power is

$$P_r = k \left[\frac{P_t G^2 \sigma \lambda^2 F^4}{R^4 L} \right]$$

where the symbols are defined as follows:

P_r - received signal power

P_t - transmitted power

G - one-way antenna gain

σ - target cross section

λ - wavelength

L loss factor (power ratio)

F - pattern-propagation factor

R - target range

k - constant depending on system of units ($= 1/(4\pi)^3$ for consistent units).

The loss factor, L, has values equal to or greater than 1, and may be considered as the product of a system loss factor and atmospheric attenuation loss, where the system loss is that due to transmission line loss and the like; thus,

$$L = L_s \times 10^{0.1A}$$

where A is the total atmospheric attenuation in decibels. Since A is a function of the range, R, of the target, the radar equation including the loss A cannot be solved directly for the range.

Two approaches to the problem are possible. If A is relatively small, say one decibel or less, the range may be calculated as if there were no atmospheric attenuation ($A = 0$). Then the atmospheric attenuation may be found for this value of range, from the appropriate graph of Figs. 1. This decibel figure may then be converted into a range ratio, and applied to the calculated range as a reduction factor. A convenient table of range ratios corresponding to decibel gains and losses is given in Table C1. The reduced range thus obtained will not be rigorously correct, because the atmospheric attenuation assumed was for a greater range than the true range, but the error will be negligible for attenuation of the order of a decibel or less.

If the attenuation is great enough to cause substantial error with the foregoing method, an iterative procedure may be employed to arrive at a more accurate range figure. The first step is to proceed as outlined above. After the corrected range is found, the attenuation corresponding to this new range figure is determined (using Figs. 1). If this figure differs substantially from the initial attenuation, a second correction is made to the range; this time it is increased by a range factor corresponding to the difference between the initial attenuation figure and the corrected figure. In principle, this in turn generates a third attenuation figure slightly larger then the second, and a third range correction may be made, a reduction corresponding to the decibel difference between the second and third attenuation figures. This process could in principle be continued indefinitely and the successive range figures obtained will converge to the correct value. In practice, one or two such corrections will be sufficient.

If very large attenuations occur, as they might at frequencies much higher than those considered here, a direct one-step graphical solution for the range may be employed. On the appropriate graph similar to Figs. 1, a plot may be made of the variation of received signal power with range according to the equation given at the beginning of this appendix. If F does not vary with range, this will simply be a curve of the form

$$P_r \text{ (decibels)} = -40 (\log_{10} R) + C.$$

The constant C is chosen so that this curve crosses the zero-decibel level at the range calculated for no atmospheric attenuation. The range at which this curve intersects the appropriate atmospheric attenuation curve is the solution of the range equation including the atmospheric attenuation.

Such a curve may be plotted readily with the assistance of the radar range factors given in Table C1. The procedure would be to determine the detection range R_1, with no atmospheric attenuation, in the usual way. A point is plotted at this range on the zero-decibel line of the appropriate graph, Figs. 1. On the one-decibel line, the point is plotted at range 0.9441 R_1, the appropriate range factor being found in the third column of the table; on the two-decibel line, the point is plotted at 0.8913 R_1; etc.

A quick method of making such calculations may be set up by plotting the attenuation curves on lin-log graph paper, with the range represented on the log scale. The curve of received power, in decibels, as a function of the range, is then simply a straight line of slope -4. This may be plotted to the correct scale on a transparent overlay which can be positioned to cross the zero-decibel level at the no-attenuation range, and the intersection with the attenuation curve may then be read off directly.

Table C1
Radar Range Factors for System Power Change from 0 to 40 Decibels (In Steps of 0.1 Decibel)

The table is intended for use with an equation of the type

$$R = k\left[\frac{P_t G^2 \lambda^2 \sigma F^4}{P_r L}\right]^{1/4} = k P^{1/4};\ \text{i.e., } R \propto P^{1/4}$$

where R is the radar range and P may be regarded as an equivalent system power variable. The table is based on the relation

$$R/R_0 = \text{antilog}\left[\frac{1}{40}\left(10 \log P/P_0\right)\right]$$

where R/R_0 is the range factor, and $10 \log P/P_0$ is the power change in decibels. P_t is transmitter power, G antenna gain, λ wavelength, σ target cross section, L loss factor, F pattern-propagation factor, and P_r received echo power.

Range factors for power changes greater than 40 db can be obtained from the table by the following procedure: (1) Subtract from the absolute value of the power change in db the integral multiple of 40 which results in a positive remainder less than 40. (2) Look up the range factor corresponding to the remainder; (3) Shift the decimal point one place for each 40 db subtracted, for range increase shift to the right, for decrease shift to the left. For example, the range increase for a power change of 47.3 db is 15.22, and for 87.3 it is 152.2, because for 7.3 db it is 1.522. The decrease factor for 47.3 db is 0.06569, and for 87.3 it is 0.006569, etc.

Power Change, Decibels ↓	Range Increase Factor (Decimal Point)	Range Decrease Factor (Decimal Point)	
0.0	1 0000	1 0 000	40.0
0.1	1 0058	9 943	39.9
0.2	1 0116	9 886	39.8
0.3	1 0174	9 829	39.7
0.4	1 0233	9 772	39.6
0.5	1 0292	9 716	39.5
0.6	1 0351	9 661	39.4
0.7	1 0411	9 605	39.3
0.8	1 0471	9 550	39.2
0.9	1 0532	9 495	39.1
1.0	1 0593	9 441	39.0
1.1	1 065	9 386	38.9
1.2	1 072	9 333	38.8
1.3	1 078	9 279	38.7
1.4	1 084	9 226	38.6
1.5	1 090	9 173	38.5
1.6	1 096	9 120	38.4
1.7	1 103	9 068	38.3
1.8	1 109	9 016	38.2
1.9	1 116	8 964	38.1
2.0	1 122	8 913	38.0
2.1	1 129	8 861	37.9
2.2	1 135	8 810	37.8
2.3	1 142	8 760	37.7
2.4	1 148	8 710	37.6
2.5	1 155	8 660	37.5
2.6	1 161	8 610	37.4
2.7	1 168	8 561	37.3
2.8	1 175	8 511	37.2
2.9	1 182	8 463	37.1
3.0	1 189	8 414	37.0
3.1	1 195	8 366	36.9
3.2	1 202	8 318	36.8
3.3	1 209	8 270	36.7
3.4	1 216	8 222	36.6
3.5	1 223	8 175	36.5
3.6	1 230	8 128	36.4
3.7	1 237	8 082	36.3
3.8	1 245	8 035	36.2
3.9	1 252	7 989	36.1
4.0	1 259	7 943	36.0
4.1	1 266	7 898	35.9
4.2	1 274	7 852	35.8
4.3	1 281	7 807	35.7
4.4	1 288	7 763	35.6
4.5	1 296	7 718	35.5
4.6	1 303	7 674	35.4
4.7	1 311	7 630	35.3
4.8	1 318	7 586	35.2
4.9	1 326	7 542	35.1
	Range Decrease Factor (Decimal Point)	Range Increase Factor (Decimal Point)	Decibels Power Change ↑

Power Change, Decibels ↓	Range Increase Factor (Decimal Point)	Range Decrease Factor (Decimal Point)	
5.0	1 334	7 499	35.0
5.1	1 341	7 456	34.9
5.2	1 349	7 413	34.8
5.3	1 357	7 371	34.7
5.4	1 365	7 328	34.6
5.5	1 372	7 286	34.5
5.6	1 380	7 244	34.4
5.7	1 388	7 203	34.3
5.8	1 396	7 162	34.2
5.9	1 404	7 120	34.1
6.0	1 413	7 080	34.0
6.1	1 421	7 039	33.9
6.2	1 429	6 998	33.8
6.3	1 437	6 958	33.7
6.4	1 445	6 918	33.6
6.5	1 454	6 879	33.5
6.6	1 462	6 839	33.4
6.7	1 471	6 800	33.3
6.8	1 479	6 761	33.2
6.9	1 488	6 722	33.1
7.0	1 496	6 683	33.0
7.1	1 505	6 645	32.9
7.2	1 514	6 607	32.8
7.3	1 522	6 569	32.7
7.4	1 531	6 531	32.6
7.5	1 540	6 494	32.5
7.6	1 549	6 457	32.4
7.7	1 558	6 420	32.3
7.8	1 567	6 383	32.2
7.9	1 576	6 346	32.1
8.0	1 585	6 310	32.0
8.1	1 594	6 273	31.9
8.2	1 603	6 237	31.8
8.3	1 612	6 202	31.7
8.4	1 622	6 166	31.6
8.5	1 631	6 131	31.5
8.6	1 641	6 095	31.4
8.7	1 650	6 061	31.3
8.8	1 660	6 026	31.2
8.9	1 669	5 991	31.1
9.0	1 679	5 957	31.0
9.1	1 688	5 923	30.9
9.2	1 698	5 888	30.8
9.3	1 708	5 855	30.7
9.4	1 718	5 821	30.6
9.5	1 728	5 788	30.5
9.6	1 738	5 754	30.4
9.7	1 748	5 721	30.3
9.8	1 758	5 689	30.2
9.9	1 768	5 656	30.1
	Range Decrease Factor (Decimal Point)	Range Increase Factor (Decimal Point)	Decibels Power Change ↑

Power Change, Decibels ↓	Range Increase Factor (Decimal Point)	Range Decrease Factor (Decimal Point)	
10.0	1 778	5 623	30.0
10.1	1 789	5 591	29.9
10.2	1 799	5 559	29.8
10.3	1 809	5 527	29.7
10.4	1 819	5 495	29.6
10.5	1 830	5 464	29.5
10.6	1 841	5 433	29.4
10.7	1 851	5 401	29.3
10.8	1 862	5 370	29.2
10.9	1 873	5 340	29.1
11.0	1 884	5 309	29.0
11.1	1 895	5 278	28.9
11.2	1 905	5 248	28.8
11.3	1 916	5 218	28.7
11.4	1 928	5 188	28.6
11.5	1 939	5 158	28.5
11.6	1 950	5 129	28.4
11.7	1 961	5 099	28.3
11.8	1 972	5 070	28.2
11.9	1 984	5 041	28.1
12.0	1 995	5 012	28.0
12.1	2 007	4 983	27.9
12.2	2 018	4 954	27.8
12.3	2 030	4 926	27.7
12.4	2 042	4 898	27.6
12.5	2 054	4 870	27.5
12.6	2 065	4 842	27.4
12.7	2 077	4 814	27.3
12.8	2 089	4 786	27.2
12.9	2 101	4 759	27.1
13.0	2 113	4 732	27.0
13.1	2 126	4 704	26.9
13.2	2 138	4 677	26.8
13.3	2 150	4 650	26.7
13.4	2 163	4 624	26.6
13.5	2 175	4 597	26.5
13.6	2 188	4 571	26.4
13.7	2 200	4 545	26.3
13.8	2 213	4 519	26.2
13.9	2 226	4 493	26.1
14.0	2 239	4 467	26.0
14.1	2 252	4 441	25.9
14.2	2 265	4 416	25.8
14.3	2 278	4 390	25.7
14.4	2 291	4 365	25.6
14.5	2 304	4 340	25.5
14.6	2 317	4 315	25.4
14.7	2 331	4 290	25.3
14.8	2 344	4 266	25.2
14.9	2 358	4 241	25.1
	Range Decrease Factor (Decimal Point)	Range Increase Factor (Decimal Point)	Decibels Power Change ↑

Power Change, Decibels ↓	Range Increase Factor (Decimal Point)	Range Decrease Factor (Decimal Point)	
15.0	2 371	4 217	25.0
15.1	2 385	4 193	24.9
15.2	2 399	4 169	24.8
15.3	2 413	4 145	24.7
15.4	2 427	4 121	24.6
15.5	2 441	4 097	24.5
15.6	2 455	4 074	24.4
15.7	2 469	4 050	24.3
15.8	2 483	4 027	24.2
15.9	2 497	4 004	24.1
16.0	2 512	3 981	24.0
16.1	2 526	3 959	23.9
16.2	2 541	3 936	23.8
16.3	2 556	3 913	23.7
16.4	2 570	3 890	23.6
16.5	2 585	3 868	23.5
16.6	2 600	3 846	23.4
16.7	2 615	3 824	23.3
16.8	2 630	3 802	23.2
16.9	2 645	3 780	23.1
17.0	2 661	3 758	23.0
17.1	2 676	3 737	22.9
17.2	2 692	3 715	22.8
17.3	2 707	3 694	22.7
17.4	2 723	3 673	22.6
17.5	2 738	3 652	22.5
17.6	2 754	3 631	22.4
17.7	2 770	3 610	22.3
17.8	2 786	3 589	22.2
17.9	2 802	3 569	22.1
18.0	2 818	3 548	22.0
18.1	2 835	3 528	21.9
18.2	2 851	3 508	21.8
18.3	2 867	3 487	21.7
18.4	2 884	3 467	21.6
18.5	2 901	3 447	21.5
18.6	2 917	3 428	21.4
18.7	2 934	3 408	21.3
18.8	2 951	3 388	21.2
18.9	2 968	3 369	21.1
19.0	2 985	3 350	21.0
19.1	3 003	3 330	20.9
19.2	3 020	3 311	20.8
19.3	3 037	3 292	20.7
19.4	3 055	3 273	20.6
19.5	3 073	3 255	20.5
19.6	3 090	3 236	20.4
19.7	3 108	3 217	20.3
19.8	3 126	3 199	20.2
19.9	3 144	3 181	20.1
20.0	3 162	3 162	20.0
	Range Decrease Factor (Decimal Point)	Range Increase Factor (Decimal Point)	Decibels Power Change ↑

* * *